

Histogram-based Parameter-efficient Tuning for Passive Sonar Classification

Amirmohammad Mohammadi¹, Davelle Carreiro², Alexandra Van Dine², Joshua Peebles¹

¹Department of Electrical and Computer Engineering, Texas A&M University, College Station, Texas, USA

²Massachusetts Institute of Technology Lincoln Laboratory, Lexington, Massachusetts, USA

Abstract—Parameter-efficient transfer learning (PETL) methods adapt large artificial neural networks to downstream tasks without fine-tuning the entire model. However, existing additive methods, such as adapters, sometimes struggle to capture distributional shifts in intermediate feature embeddings. We propose a novel histogram-based parameter-efficient tuning (HPT) technique that captures the statistics of the target domain and modulates the embeddings. Experimental results on three downstream passive sonar datasets (ShipsEar, DeepShip, VTUAD) demonstrate that HPT outperforms conventional adapters. Notably, HPT achieves 91.8% vs. 89.8% accuracy on VTUAD. Furthermore, HPT trains faster and yields feature representations closer to those of fully fine-tuned models. Overall, HPT balances parameter savings and performance, providing a distribution-aware alternative to existing adapters and shows a promising direction for scalable transfer learning in resource-constrained environments. The code is publicly available: https://github.com/Advanced-Vision-and-Learning-Lab/HLAST_DeepShip_ParameterEfficient.

1. INTRODUCTION

Transfer learning from pre-trained models has shown performance improvements and faster convergence compared to training from scratch, especially in scenarios with limited labeled data [1]. However, fine-tuning all parameters of large-scale models for each downstream task is resource-intensive, as a new set of weights must be tuned and stored for each target task, making this impractical for edge device applications [2]. To address these issues, parameter-efficient transfer learning (PETL) methods [3] have been developed, where the pre-trained model’s weights are kept frozen while a smaller number of parameters are used to adapt to the target task. Many PETL techniques are based on methods such as inserting adapters [4], adding prompt tokens [5], or applying low-rank decompositions [6].

Although these approaches have demonstrated strong empirical performance, some tasks may benefit from more distribution-aware adaptation [7]. In particular, acoustic data can face distribution mismatches due to diverse recording conditions and environmental factors [8]. Mitigating these mismatches using a distribution-aware adaptation is one potential approach to improve generalizability. Underwater acoustic recognition has various applications in marine environments such as search and rescue, seabed mapping, and shipping traffic monitoring [9], [10]. In this work, a histogram-based parameter-efficient tuning (HPT) method that learns to represent intermediate embeddings as feature distributions is proposed. It is empirically validated that HPT outperforms conventional adapters in accuracy

DISTRIBUTION STATEMENT A. Approved for public release. Distribution is unlimited. This material is based upon work supported by the Under Secretary of Defense for Research and Engineering under Air Force Contract No. FA8702-15-D-0001 or FA8702-25-D-B001. Any opinions, findings, conclusions or recommendations expressed in this material are those of the author(s) and do not necessarily reflect the views of the Under Secretary of Defense for Research and Engineering. ©2025 Massachusetts Institute of Technology. Delivered to the U.S. Government with Unlimited Rights, as defined in DFARS Part 252.227-7013 or 7014 (Feb 2014). Notwithstanding any copyright notice, U.S. Government rights in this work are defined by DFARS 252.227-7013 or DFARS 252.227-7014 as detailed above. Use of this work other than as specifically authorized by the U.S. Government may violate any copyrights that exist in this work.

while offering a favorable parameter trade-off. This method’s scalable potential is also shown—allowing a balance between computational cost and performance in resource-constrained environments.

2. RELATED WORK

Following [3], PETL methods can be categorized into four groups: additive, selective, reparameterized, and hybrid. Additive methods such as adapters [4], [11] introduce small trainable modules (e.g., bottleneck layers) into the pre-trained model, leaving original parameters frozen. Similarly, soft prompts like prefix-tuning [12] and prompt-tuning [5] add learnable vectors to the input sequence. On the other hand, selective methods only update a subset of existing parameters, such as BitFit [13], which tunes only a set of bias terms. Reparameterized methods (e.g., low-rank adaptation (LoRA) [6]) learn compact updates that can be merged back into the original weights at inference. Scaling and shifting features (SSF) [7] inserts additional layers after every major operation to apply linear transformations to the features (scale and shift parameters can be merged back into base weights at inference). Finally, hybrid methods unify multiple strategies, acknowledging that different tasks may require different forms of adaptation. For example, UniPELT [14] integrates LoRA, prefix-tuning, and adapters in each transformer block, using a gating mechanism to modulate their relative contributions. PETL research has mostly focused on natural language processing (NLP) or vision tasks, while acoustic-specific PETL solutions remain less explored—even though such data can exhibit unique distribution shifts.

SSF [7] assumes that the upstream datasets and downstream datasets have different data distributions [15] thereby justifying a reparameterized linear transformation to alleviate this mismatch. Similarly, this manuscript proposes an additive non-linear transformation which can capture feature statistics. Building on the simplicity and modularity of additive methods, this work seeks to advance beyond conventional adapters by incorporating distribution-aware mechanisms using histogram layers [16]. This approach focuses on passive sonar in underwater environmental monitoring [17] as PETL approaches in this domain have remained comparatively understudied, while requiring the handling of complex acoustic signatures. Using histogram layers for passive sonar has been shown to improve performance of convolutional neural networks [18]. This work shows how PETL can be extended to address such specialized tasks, broadening the applicability of this area of research.

3. METHOD

The original histogram layer [16] approach was used for 2-dimensional data (i.e., images). The histogram layer herein is adapted for 1-dimensional data (i.e., sequences) and incorporates this method parallel to the multi-head self-attention (MHSA) sublayer of the transformer architecture. Let $\mathbf{X} \in \mathbb{R}^{N \times D}$ denote the input to the histogram layer, where D is the feature dimension (e.g., 768) and N is the sequence length (i.e., number of patches). The histogram layer first applies two successive 1×1 convolutions. The first convolution projects \mathbf{X}

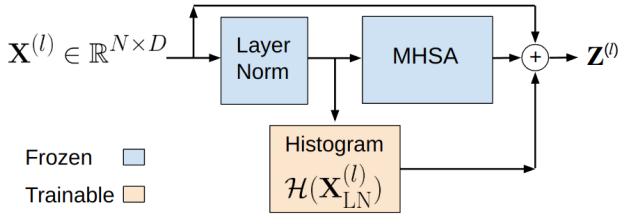


Fig. 1: Integration of the histogram layer into the transformer architecture. The histogram layer operates in parallel with the MHSA sublayer.

onto B channels (i.e., bins), with the learnable biases serving as bin centers $\{\mu_b\}_{b=1}^B$. The second, implemented as a grouped convolution, learns bin-specific widths $\{\gamma_b\}_{b=1}^B$. For each feature value x , a radial basis function (RBF) computes its assignment to the b th bin as shown in (1):

$$y_b(x) = \exp\left(-\gamma_b^2(x - \mu_b)^2\right), \quad (1)$$

Responses are then normalized across bins so the contribution of each descriptor is in the range of $[0, 1]$. Specifically, the normalized bin response is defined in (2):

$$\hat{r}_b(x) = \frac{\exp\left(-\gamma_b^2(x - \mu_b)^2\right)}{\sum_{b'=1}^B \exp\left(-\gamma_{b'}^2(x - \mu_{b'})^2\right) + \epsilon}, \quad b = 1, \dots, B, \quad (2)$$

where ϵ is a small constant (10^{-6}) added for numerical stability to prevent division by zero. These normalized responses are then aggregated via adaptive average pooling along the sequence dimension to capture the overall statistical distribution. Equation (3) denotes the pooling and broadcasting:

$$\mathcal{H}(\mathbf{X}) = \text{Broadcast}\left\{\mathcal{P}\left[\{\hat{r}_b(x)\}_{b=1}^B\right]\right\}. \quad (3)$$

Here, $\mathcal{P}(\cdot)$ is the adaptive average pooling operation that reduces the variable-length responses to a fixed-size summary, and $\text{Broadcast}(\cdot)$ replicates this summary across all patches so that every patch is augmented with the same statistical context. Given layer-normalized features \mathbf{X}_{LN} and the histogram-based representation $\mathcal{H}(\mathbf{X})$, the updated output (as shown in Fig. 1) is computed as:

$$\mathbf{Z} = \mathbf{X} + \text{MHSA}(\mathbf{X}_{\text{LN}}) + \mathcal{H}(\mathbf{X}_{\text{LN}}). \quad (4)$$

While the described approach applies the histogram layer after layer normalization and incorporates its output alongside the MHSA sublayer’s features, other configurations are possible. For instance, the histogram layer may be applied after the feed-forward network (FFN) sublayer. Histogram features were added alongside MHSA to inform the self-attention process with distributional statistics. In practice, histogram features may be introduced at multiple portions of the network (in parallel and/or residual). The proposed HPT allows for different configurations that can be leveraged for flexible adaptation strategies and potentially improve performance across various tasks.

4. EXPERIMENTS

An evaluation of the histogram-based adaptation approach against full fine-tuning, linear probing, and adapter methods is presented in this section. Initially, HPT is compared with adapters since both belong to the same additive category. The Audio Spectrogram Transformer

(AST) [19] (built upon a Vision Transformer (ViT) [20] with 86M parameters) which is pre-trained on ImageNet [21] and AudioSet [22] is used. Experiments were conducted on three passive sonar datasets: ShipsEar [23], DeepShip [24], and vessel type underwater acoustic data (VTUAD) [25]. Input is a 128-dimensional log Mel-frequency spectrogram [26] with a window length of 2048 and a hop length of 512. The learning rate is set to $1e-5$ for full fine-tuning and $1e-3$ for all other methods. The optimizer is AdamW and the batch size is 64 for ShipsEar and DeepShip, and 256 for VTUAD. The maximum epoch number is set to 200 and early stopping is implemented to stop training if there is no improvement in the validation loss after 20 epochs. The reported accuracies are based on the unseen test split. Mean accuracy (%) along with standard deviations (subscripted) from three runs of random initialization are reported. The histogram convolutional layers use PyTorch’s default initialization (Kaiming method), while the adapters are zero-initialized. Experiments were completed on an A100 GPU.

Three adapter configurations are considered, defined by reduction rates of 256, 128, and 64. Three histogram configurations are considered, defined by 4, 8, and 16 bins. Initially, a shared-weights setting where the same adapter or histogram parameters are used across all transformer layers is applied. This range of configurations is chosen to systematically explore the trade-off between accuracy and parameter efficiency, so that both lightweight and more expressive modules are compared. Table 1 presents results under this scenario, showing that the histogram configurations outperform adapters. More parameters leads to a higher accuracy, thus indicating the scalability of the HPT method.

Table 1: Mean classification accuracy (%) with subscripted standard deviations and total trainable parameters under the shared-weights setting. The best accuracies are shown in **bold**. In the Params column, the left number corresponds to DeepShip, and the right number corresponds to ShipsEar and VTUAD.

Method	DeepShip	ShipsEar	VTUAD	Params
Full fine tune	70.0 _{1.0}	60.0 _{1.4}	96.3_{0.1}	86.9M/86.9M
Linear probe	66.2 _{0.8}	56.4 _{2.5}	79.9 _{0.2}	4.9K/5.6K
Adapter (256)	67.1 _{0.7}	56.5 _{1.7}	83.8 _{0.4}	10.2K/11.0K
Adapter (128)	66.1 _{0.9}	56.8 _{0.6}	83.3 _{0.2}	14.9K/15.6K
Adapter (64)	66.7 _{0.5}	56.2 _{0.6}	83.2 _{0.1}	24.1K/24.8K
HPT (4)	69.8 _{0.6}	52.8 _{2.2}	85.0 _{0.1}	7.9K/8.7K
HPT (8)	70.4_{0.6}	53.9 _{1.4}	86.4 _{0.5}	11.0K/11.8K
HPT (16)	70.0 _{0.2}	60.1_{3.1}	88.1 _{0.2}	17.2K/18.0K

Since full fine-tuning accuracy was not achieved for VTUAD, the shared-weight restriction was removed, allowing each layer to have its own adapter or histogram parameters. Table 2 shows that with non-shared weights, histogram configurations more closely approach full fine-tuning accuracy. Allowing each layer to fine-tune its own histogram parameters provides more control over layer-specific distributional alignment. Figure 2 visualizes histogram scalable performance with the number of bins, while performance of the adapters saturates.

Training convergence between histograms and adapters is compared in Fig. 3, where eight loss curves are presented with a reduction rate of 64 and 16 histogram bins. While convergence speed is similar in ShipsEar and DeepShip, the histograms converge more rapidly and stably than adapters in VTUAD, showing the benefits of distributional representation. One possible explanation is that VTUAD is much larger than the other datasets (about 6x), and this makes histograms

Table 2: Mean classification accuracy (%) and parameters on VTUAD under non-shared weights settings. Standard deviations are subscripted. The best accuracy is shown in **bold**.

Method	VTUAD Accuracy	Params
Full fine tune	96.3_{0.1}	86.9M
Linear probe	79.9 _{0.2}	5.6K
Adapter (256)	89.6 _{0.2}	70.2K
Adapter (128)	89.8 _{0.3}	125.0K
Adapter (64)	89.1 _{0.5}	236.0K
HPT (4)	89.6 _{0.2}	42.6K
HPT (8)	90.3 _{0.3}	79.6K
HPT (16)	91.8 _{0.4}	153.0K

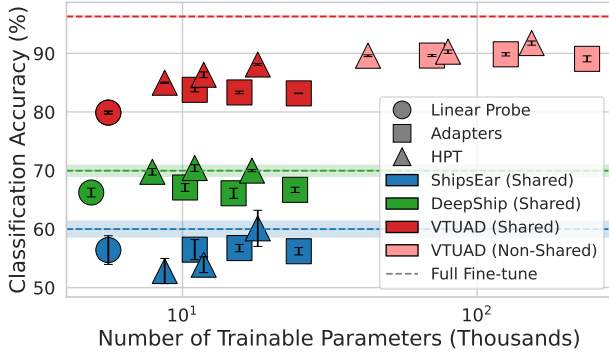


Fig. 2: Scalability comparison of HPT and adapters. HPT performance increases with the number of bins if it has not already reached the full fine-tuning accuracy.

particularly advantageous for summarizing vast amounts of data. Also, we attribute faster convergence partly to PyTorch’s default Kaiming initialization of histograms, which maintains variance [27] better than zero-initialized adapters. This helps to learn features quickly compared to zero-initialized scenarios, which begin with no variance and can suffer from slower learning. However, while this initialization can drive rapid initial convergence, it might also limit adapter performance.

Figure 4 visualizes feature similarity analysis. Each compares the layer-wise similarity of linear probe, adapter and histogram methods to the fully fine-tuned baseline. It is observed that histograms retain higher similarity, indicating that they capture a higher level of semantic representation than adapters, while adapters sometimes even achieve a lower similarity than linear probing. It is observed that in the early layers, all methods preserve low-level features, thereby maintaining high similarity. Progressing into the mid-layers, where more specialized abstractions occur, the adapter approach deviates more strongly, causing similarity to drop. In contrast, histograms—by summarizing the distribution—retain closer alignment with the baseline’s intermediate features, though some divergence still appears. Finally, at the upper layers, both methods converge somewhat again, as the model refines representations for the final classification task; this leads to a slight rebound in similarity, suggesting that certain task-specific semantics are being aligned.

To compare HPT with other related works, LoRA [6] and SSF [7] were integrated into AST. For LoRA, the mechanism is applied to the query component with a rank of 6 and 12, while α is set to 1 so the scaling factor becomes 1/6 and 1/12, respectively. For SSF, six layers were inserted at these points: after the first LayerNorm, after the QKV projection, after the final projection in the attention sub-layer, after the second LayerNorm, after the first and second fully connected

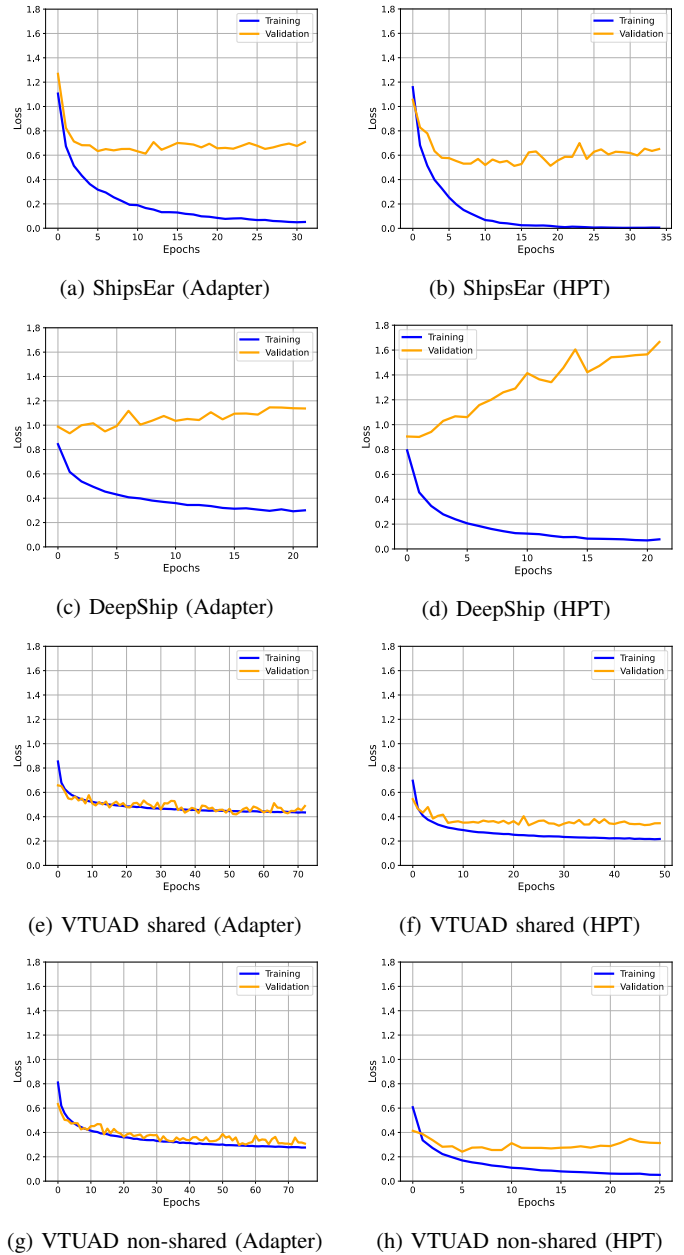


Fig. 3: Loss convergence for adapters (left column) and HPT (right column). HPT exhibits faster and more stable convergence for the VTUAD dataset.

layers. An element-wise affine transformation $x \leftarrow \text{scale} \odot x + \text{shift}$ is learned. Shared settings across all experiments are used so that the performance differences arise exclusively from the fine-tuning mechanism itself with minimal parameter footprint. It should be noted that the SSF six layers are distinct in the block.

The results in Table 3 show varying strengths across different fine-tuning strategies and datasets. On DeepShip, HPT with 8 bins achieves the highest accuracy (70.4%), surpassing LoRA and SSF. This indicates that distribution-based tuning can effectively capture the relevant acoustic characteristics of mid-scale datasets. In contrast, on VTUAD, the larger dataset size favors SSF with six layers (92.2%). Meanwhile, ShipsEar shows relatively more variability in performance across all methods, likely reflecting its unique acoustic characteristics

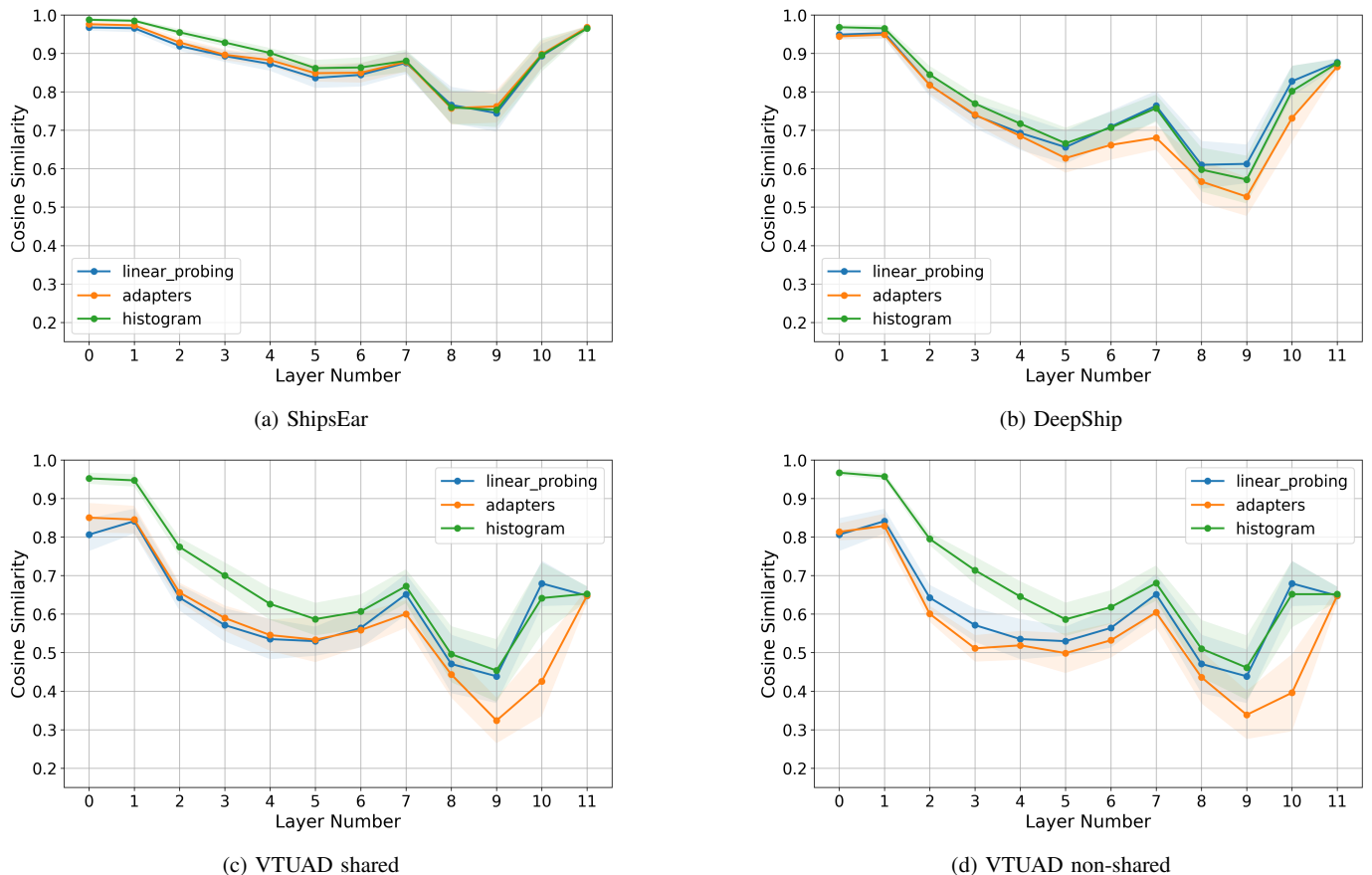


Fig. 4: Layer-wise feature similarity for ShipsEar, DeepShip, VTUAD (shared), and VTUAD (non-shared). Histograms maintain closer similarity with the fully fine-tuned model’s representations.

Table 3: Accuracy (%) and trainable parameters for different shared fine-tuning methods. Standard deviations are subscripted. The best accuracies are shown in **bold**. In the Params column, the right number corresponds to ShipsEar and VTUAD and the left number corresponds to DeepShip.

Method	DeepShip	ShipsEar	VTUAD	Params
Full fine tune	70.0 _{1.0}	60.0 _{1.4}	96.3 _{0.1}	86.9M/86.9M
Linear probe	66.2 _{0.8}	56.4 _{2.5}	79.9 _{0.2}	4.9K/5.6K
LoRA				
rank of 6	68.0 _{1.5}	45.3 _{2.1}	82.6 _{0.8}	14.1K/14.9K
rank of 12	67.8 _{0.5}	47.9 _{1.1}	84.3 _{0.6}	23.3K/24.1K
SSF				
LayerNorm	66.2 _{0.2}	56.9 _{0.3}	86.3 _{0.3}	6.4K/7.2K
MHSA	67.9 _{0.7}	55.4 _{1.2}	90.5 _{0.5}	12.5K/13.3K
MHSA & FFN	68.4 _{0.7}	54.8 _{1.1}	92.2 _{0.3}	21.8K/22.5K
HPT (ours)				
4 bins MHSA	69.8 _{0.6}	52.8 _{2.2}	85.0 _{0.1}	7.9K/8.7K
8 bins MHSA	70.4 _{0.6}	53.9 _{1.4}	86.4 _{0.5}	11.0K/11.8K
16 bins MHSA	70.0 _{0.2}	60.1 _{3.1}	88.1 _{0.2}	17.2K/18.0K

and smaller overall dataset size. This reinforces the idea that no single tuning approach universally dominates; rather, the best choice may depend on both the data scale and the acoustic properties of the target domain.

While the proposed HPT approach demonstrates strong performance,

there remain some limitations and avenues for further research. First, HPT’s efficacy can depend on hyper-parameters such as the number of bins and the layer injection strategy. Finding the optimal configuration may require extensive experimentation. Second, HPT’s reliance on distributional modeling could become less beneficial for tasks with extremely sparse data, as the histogram estimates might not adequately capture the feature distributions. Addressing this would likely involve adaptive binning strategies to regularize histogram layers.

5. CONCLUSION

In this work, a novel parameter-efficient tuning method, a histogram layer integrated into the transformer architecture, is introduced. Experiments on three passive sonar datasets demonstrated that HPT not only achieves competitive and superior accuracy compared to conventional adapters, but does so with a favorable parameter trade-off and improved convergence. Future work could explore different binning functions to capture a richer distribution. Another promising direction lies in combining HPT with other PETL techniques (e.g., LoRA), by joint optimization to leverage complementary benefits. Finally, integrating HPT with diffusion-based approaches could lead to a more scalable framework for efficient training of generative models. This work aims to pave the way for more distribution-aware techniques in efficient learning strategies.

6. ACKNOWLEDGMENT

Portions of this research were conducted with the advanced computing resources provided by Texas A&M High Performance Research Computing.

REFERENCES

- [1] T. Pégeot, I. Kucher, A. Popescu, and B. Delezoide, “A comprehensive study of transfer learning under constraints,” in *Proceedings of the IEEE/CVF International Conference on Computer Vision*, 2023, pp. 1148–1157.
- [2] U. Evci, V. Dumoulin, H. Larochelle, and M. C. Mozer, “Head2toe: Utilizing intermediate representations for better transfer learning,” in *International Conference on Machine Learning*. PMLR, 2022, pp. 6009–6033.
- [3] Z. Han, C. Gao, J. Liu, J. Zhang, and S. Q. Zhang, “Parameter-efficient fine-tuning for large models: A comprehensive survey,” *arXiv preprint arXiv:2403.14608*, 2024.
- [4] N. Houlsby, A. Giurgiu, S. Jastrzebski, B. Morrone, Q. De Laroussilhe, A. Gesmundo, M. Attariyan, and S. Gelly, “Parameter-efficient transfer learning for nlp,” in *International conference on machine learning*. PMLR, 2019, pp. 2790–2799.
- [5] B. Lester, R. Al-Rfou, and N. Constant, “The power of scale for parameter-efficient prompt tuning,” *arXiv preprint arXiv:2104.08691*, 2021.
- [6] E. J. Hu, Y. Shen, P. Wallis, Z. Allen-Zhu, Y. Li, S. Wang, L. Wang, and W. Chen, “Lora: Low-rank adaptation of large language models,” *arXiv preprint arXiv:2106.09685*, 2021.
- [7] D. Lian, D. Zhou, J. Feng, and X. Wang, “Scaling & shifting your features: A new baseline for efficient model tuning,” *Advances in Neural Information Processing Systems*, vol. 35, pp. 109–123, 2022.
- [8] A. Mesaros, T. Heittola, and T. Virtanen, “A multi-device dataset for urban acoustic scene classification,” *arXiv preprint arXiv:1807.09840*, 2018.
- [9] A. Testolin, D. Kipnis, and R. Diamant, “Detecting submerged objects using active acoustics and deep neural networks: A test case for pelagic fish,” *IEEE Transactions on Mobile Computing*, vol. 21, no. 8, pp. 2776–2788, 2020.
- [10] B. Beckler, A. Pfau, M. Orescanin, S. Atchley, N. Villemez, J. E. Joseph, C. W. Miller, and T. Margolina, “Multilabel classification of heterogeneous underwater soundscapes with bayesian deep learning,” *IEEE Journal of Oceanic Engineering*, vol. 47, no. 4, pp. 1143–1154, 2022.
- [11] J. He, C. Zhou, X. Ma, T. Berg-Kirkpatrick, and G. Neubig, “Towards a unified view of parameter-efficient transfer learning,” *arXiv preprint arXiv:2110.04366*, 2021.
- [12] X. L. Li and P. Liang, “Prefix-tuning: Optimizing continuous prompts for generation,” *arXiv preprint arXiv:2101.00190*, 2021.
- [13] E. B. Zaken, S. Ravfogel, and Y. Goldberg, “Bitfit: Simple parameter-efficient fine-tuning for transformer-based masked language-models,” *arXiv preprint arXiv:2106.10199*, 2021.
- [14] Y. Mao, L. Mathias, R. Hou, A. Almahairi, H. Ma, J. Han, W.-t. Yih, and M. Khabsa, “Unipelt: A unified framework for parameter-efficient language model tuning,” *arXiv preprint arXiv:2110.07577*, 2021.
- [15] B. Sun, J. Feng, and K. Saenko, “Return of frustratingly easy domain adaptation,” in *Proceedings of the AAAI conference on artificial intelligence*, vol. 30, 2016.
- [16] J. Peeples, W. Xu, and A. Zare, “Histogram layers for texture analysis,” *IEEE Transactions on Artificial Intelligence*, vol. 3, no. 4, pp. 541–552, 2021.
- [17] S. Tian, D. Chen, H. Wang, and J. Liu, “Deep convolution stack for waveform in underwater acoustic target recognition,” *Scientific reports*, vol. 11, no. 1, p. 9614, 2021.
- [18] J. Ritu, E. Barnes, R. Martell, A. Van Dine, and J. Peeples, “Histogram layer time delay neural networks for passive sonar classification,” in *2023 IEEE Workshop on Applications of Signal Processing to Audio and Acoustics (WASPAA)*. IEEE, 2023, pp. 1–5.
- [19] Y. Gong, Y.-A. Chung, and J. Glass, “Ast: Audio spectrogram transformer,” *arXiv preprint arXiv:2104.01778*, 2021.
- [20] H. Touvron, M. Cord, M. Douze, F. Massa, A. Sablayrolles, and H. Jégou, “Training data-efficient image transformers & distillation through attention,” in *International conference on machine learning*. PMLR, 2021, pp. 10347–10357.
- [21] J. Deng, W. Dong, R. Socher, L.-J. Li, K. Li, and L. Fei-Fei, “Imagenet: A large-scale hierarchical image database,” in *2009 IEEE conference on computer vision and pattern recognition*. Ieee, 2009, pp. 248–255.
- [22] J. F. Gemmeke, D. P. Ellis, D. Freedman, A. Jansen, W. Lawrence, R. C. Moore, M. Plakal, and M. Ritter, “Audio set: An ontology and human-labeled dataset for audio events,” in *2017 IEEE international conference on acoustics, speech and signal processing (ICASSP)*. IEEE, 2017, pp. 776–780.
- [23] D. Santos-Domínguez, S. Torres-Guijarro, A. Cardenal-López, and A. Pena-Gimenez, “Shipsear: An underwater vessel noise database,” *Applied Acoustics*, vol. 113, pp. 64–69, 2016.
- [24] M. Irfan, Z. Jiangbin, S. Ali, M. Iqbal, Z. Masood, and U. Hamid, “Deepship: An underwater acoustic benchmark dataset and a separable convolution based autoencoder for classification,” *Expert Systems with Applications*, vol. 183, p. 115270, 2021.
- [25] L. C. F. Domingos, P. E. Santos, P. S. M. Skelton, R. S. A. Brinkworth, and K. Sammut, “An investigation of preprocessing filters and deep learning methods for vessel type classification with underwater acoustic data,” *IEEE Access*, vol. 10, pp. 117582–117596, 2022.
- [26] Q. Kong, C. Yu, Y. Xu, T. Iqbal, W. Wang, and M. D. Plumbley, “Weakly labelled audioset tagging with attention neural networks,” *IEEE/ACM Transactions on Audio, Speech, and Language Processing*, vol. 27, no. 11, pp. 1791–1802, 2019.
- [27] K. He, X. Zhang, S. Ren, and J. Sun, “Delving deep into rectifiers: Surpassing human-level performance on imagenet classification,” in *Proceedings of the IEEE international conference on computer vision*, 2015, pp. 1026–1034.